

Fig. 4 Surface pressure and skin friction distributions for CAST-7 aerofoil, $M_\infty = 0.70$, $\alpha = 4.59$ deg, $Re_\infty = 5.96 \times 10^6$, grid 257×61 : —, model 1; ····, model 2; ----, model 3; - · - ·, model 4; ○ ○ ○, experiment.

For the three cases computed here, all of the four models predicted the separation point at approximately the same location. Reattachment points are same for models 1 and 2 but differ a little for models 3 and 4 in the first two cases. In the third case all of the models predicted the same separation and reattachment points. An overall good C_f distribution has been obtained by all of the four models. The basic criteria to compute shock-induced separated flows are the replacement of the wall shear stress by its local maximum value inside the bubble, and the replacement of the normal distance from the wall by the normal distance from the minimum velocity line in models 1 and 2 and from the back flow edge in models 3 and 4. Fine grid (495×91) computation (results not shown here) also showed similar behavior. This study also suggests that the flow between the wall and the minimum velocity line inside the bubble can be treated as laminar, and outside the minimum velocity line the flow behaves like attached flow.

We infer from this analysis that algebraic turbulence models, in general, predict stronger shock, but the separation bubble at the foot of the shock and the skin-friction distribution can be predicted well by any of the four models described earlier. As pointed out by Bradshaw,¹ for transonic flows, the normal pressure gradient is not negligible inside the boundary-layer and so does not obey the boundary-layer assumption. In the present algorithm this assumption has been used only through the turbulence model. The velocity gradient produced due to this, in principle, leads to extra production of turbulence through the product of mean velocity gradient and turbulent shear stress. Prediction of correct wall shear stress by the present models merely implies correct prediction of mean velocity profiles and not the velocity gradients. In rapidly growing flows near separation, where normal pressure gradients affect the mean velocity gradient, one cannot expect an acceptable pressure distribution. So, for better results in both skin friction and pressure distribution, turbulence models should be developed for Navier-Stokes computations without any boundary-layer type of approximations.

References

- ¹Bradshaw, P., "Turbulence: The Chief Outstanding Difficulty of Our Subject," *Experiments in Fluids*, Vol. 16, No. 2, 1994, pp. 203–216.
- ²Cebeci, T., Smith, A. M. O., and Mosinski, G., "Calculation of Compressible Adiabatic Turbulent Boundary Layers," *AIAA Journal*, Vol. 8, No. 11,

1970, pp. 1974–1982.

³Cebeci, T., and Smith, A. M. O., "Analysis of Turbulent Boundary Layers," *Applied Mathematics and Mechanics*, Academic, New York, 1974.

⁴Baldwin, B. S., and Lomax, H., "Thin Layer Approximation and Algebraic Model for Separated Turbulent Flows," AIAA Paper 78-257, Jan. 1978.

⁵Swanson, R. C., and Turkel, E., "A Multistage Time Stepping Scheme for the Navier-Stokes Equations," AIAA Paper 85-0035, Jan. 1985.

⁶Müller, B., and Rizzi, A., "Runge-Kutta Finite Volume Simulation of Laminar Transonic Flow over a NACA-0012 Airfoil Using the Navier-Stokes Equations," Aeronautical Research Inst. of Sweden, FFA TN 1986-60, Stockholm, Sweden, Nov. 1986.

⁷Johnston, L. J., "Solution of the Reynolds-averaged Navier-Stokes Equations for Transonic Airfoil Flows," *Aeronautical Journal*, Vol. 95, No. 948, 1991, pp. 253–273.

⁸Ni, R. H., "A Multiple Grid Scheme for Solving the Euler Equations," *AIAA Journal*, Vol. 20, No. 11, 1992, pp. 1565–1571.

⁹Hall, M. G., "Cell Vertex Multigrid Scheme for Solution of Euler Equations," RAE-TM-Aero-2029, March 1985.

¹⁰Chakrabarty, S. K., "Numerical Solution of Navier-Stokes Equations for Two-Dimensional Viscous Compressible Flows," *AIAA Journal*, Vol. 27, No. 7, 1989, pp. 843, 844.

¹¹Chakrabarty, S. K., "Vertex Based Finite Volume Solution of the Two-Dimensional Navier-Stokes Equations," *AIAA Journal*, Vol. 28, No. 10, 1990, pp. 1829–1831.

¹²Radespiel, R., "A Cell Vertex Multigrid Method for the Navier-Stokes Equations," NASA TM 101557, Jan. 1989.

¹³Chakrabarty, S. K., "A Finite Volume Nodal Point Scheme for Solving Two Dimensional Navier-Stokes Equations," *Acta Mechanica*, Vol. 84, No. 1–2, 1990, pp. 139–153.

¹⁴Goldberg, U. C., "Separated Flow Treatment with a New Turbulence Model," *AIAA Journal*, Vol. 24, No. 10, 1986, pp. 1711–1713.

¹⁵Johnson, D. A., and King, L. S., "A New Turbulence Closure Model for Boundary Layer Flows with Strong Adverse Pressure Gradients and Separation," AIAA Paper 84-0175, Jan. 1984.

¹⁶Cook, P. H., McDonald, M. A., and Firmin, M. C. P., "Aerofoil RAE-2822—Pressure Distributions and Boundary Layer and Wake Measurements," AGARD-AR-138, May 1979, pp. A6-1–A6-77.

¹⁷Harris, C. D., "Two Dimensional Aerodynamic Characteristics of the NACA 0012 Airfoil in the Langley 8-foot Transonic Pressure Tunnel," NASA TM 81927, April 1981.

¹⁸Stanewsky, E., Puffert, W., Müller, R., and Bateman, T. E. B., "Supercritical Aerofoil CAST-7 Surface Pressure, Wake and Boundary Layer Measurements," AGARD-AR-138, May 1979, pp. A3-1–A3-35.

Determination of Starting Shock Velocity in Supersonic Wind Tunnel

Peter J. Disimile*

University of Cincinnati, Cincinnati, Ohio 45221
and

Norman Toy†

University of Surrey,
Guildford GU2 5XH, England, United Kingdom

Introduction

IN the case of many high-speed facilities, the nominal experimental run time is often on the order of seconds or minutes before the facility air is exhausted. During this time the tunnel parameters have to stabilize before measurements are taken, and it is this time period that is very important to the tunnel operating conditions. For supersonic/hypersonic tunnels this time period is related

Received July 29, 1994; revision received Jan 6, 1995; accepted for publication Jan. 6, 1995. Copyright © 1995 by Peter J. Disimile and Norman Toy. Published by the American Institute of Aeronautics and Astronautics, Inc., with permission.

*Bradley Jones Associate Professor, Department of Aerospace Engineering and Engineering Mechanics. Member AIAA.

†Professor in Fluid Mechanics, Department of Civil Engineering.

to the passing of the starting shock through the working section, and in many applications this has to be inferred from pressure measurements. Although these techniques are well established, they are generally only point measurements. In the case of an inclined shock, probe or tap location would bias the measurement; therefore, a full-field technique would be advantageous. It is this particular area that the technique of using liquid crystals is to address, in particular to evaluate the speed of the shock wave as the tunnel is started. The method relies upon coating the surface of the tunnel wall with a thin layer of liquid crystal¹⁻³ and illuminating the surface with white light while viewing with a color charge-coupled device (CCD) camera.

Supersonic Wind-Tunnel Facility

The development of a new technique for the determination of stable conditions within a supersonic wind-tunnel facility was performed at the University of Cincinnati. This tunnel is of an intermittent blowdown configuration with a working test section of 15.24×16.54 cm. The Mach numbers in the tunnel can be varied between 1.4 and 3.8 through the use of an asymmetric block arrangement. This nozzle configuration produces an inclined starting shock.

Compressed air used to operate the tunnel is stored in tanks with a total storage capacity of 60.9 m^3 and a working pressure of 13.79 MPa. This storage capability allows for run times on the order of 4 min at Mach 2.0. To assure a constant stagnation pressure, a series of regulating valves is used to decrease the tank pressure to the required pressure for proper tunnel operation. Reynolds numbers between 27.8 to $82.7 \times 10^6/\text{m}$ can be realized in this Mach number range.

Tunnel parameters measured include the manifold, stagnation and static pressures, heat exchanger air-in and air-out temperatures, and the stagnation temperature. For this particular experiment the lower nozzle block in the tunnel was set to produce a freestream Mach number of 2.0.

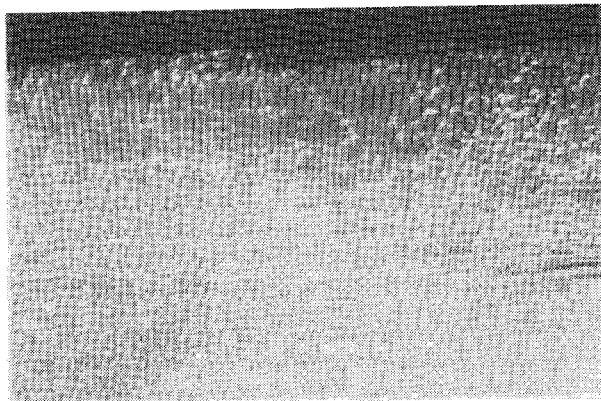


Fig. 1 Photograph of the starting shock as it passes down the tunnel (flow is from right to left).

Methodology

Liquid crystals of the type CNR2 were applied in a thin layer, on the order of $10 \mu\text{m}$, to the side wall of the test section, which was first black anodized. This coating was then illuminated with two 300-W quartz-halogen light sources while a super VHS (SVHS) color CCD video camera, providing red, green, and blue (RGB) output, was positioned normal to the crystals. At present, postprocessing of the video signal has been achieved by recording the passing of the shock over the crystals via the color change and then employing video digitization to individual frames. The digitized frames were then analyzed using hue-saturation-intensity (HSI).

Figure 1 shows the starting shock captured by photographing one digitized frame from the SVHS video tape. The shock produces a variation in the local shear stress,⁴⁻⁶ and this causes the crystals to exhibit different hue (color) according to the level of the shear, with red being at the lower stress level and blue at the higher. Also shown in this figure is the asymmetry of the shock, and this is due to the asymmetrical wall liner that is positioned upstream of the working section. (However, it should be noted that this figure has been taken from a video tape, suffers from some degradation, and is shown here for illustrative purposes only, whereas the digitizing process acts upon the frame image.)

Analysis

The analysis of the frames captured on tape was achieved by setting a sample window and digitizing a number of frames containing evidence of the passing of the shock structure. Since the video frames were captured at a known rate, 30 Hz, the analysis of the movement of this shock position provided the velocity of the shock wave down the tunnel.

Figures 2-4 show hue contours and how they change as the shock passes through the working section. These three figures were taken as the inclined starting shock traveled through the test section and are shown here, not as consecutive frames, but as every second frame for clarity. In these figures the approximate position of the shock is estimated to be the region of minimum shear stress and is represented by contours of hue = 0.09.

The velocity of the shock as it passes down the tunnel was determined from an analysis of the location of this hue contour and knowing the time between the frames, allowing for the linear scale per pixel. For example, the video digitizing speed was set at 30 frames per second, giving 33 ± 0.001 ms between frames. For consecutive frames the average distance traveled by the shock from one frame to the next was approximately 35 pixels, with a scale factor of 0.19 ± 0.02 mm/pixel, giving a shock velocity of $35 \times 0.19/0.033$ mm/s, that is, 202 ± 20 mm/s or approximately 0.20 ± 0.02 m/s. Once the shock had passed through this test section, the static pressure dropped from 11.11 to 4.85 psia.

In addition to the shock location and speed, its angle may also be determined from the relative positions of the shock at each stage in its traverse. In this particular case the shock is approximately 35 ± 3 deg to the freestream flow direction, as measured by the pixel locations of the shock front.

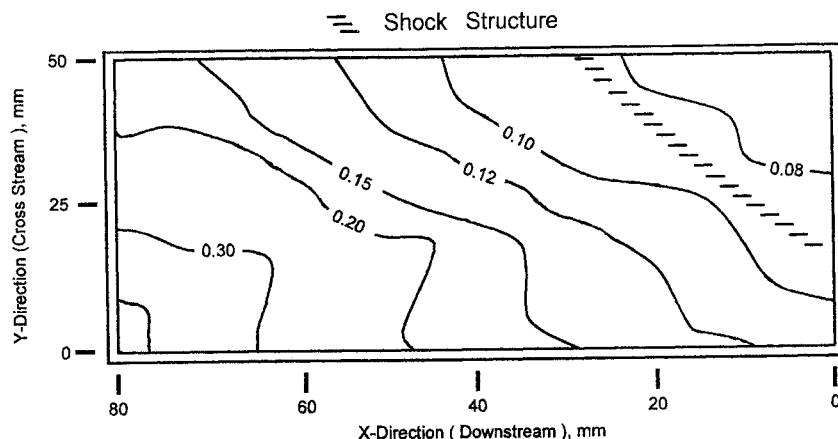


Fig. 2 Contours of constant hue showing the location of a shock line at time T .

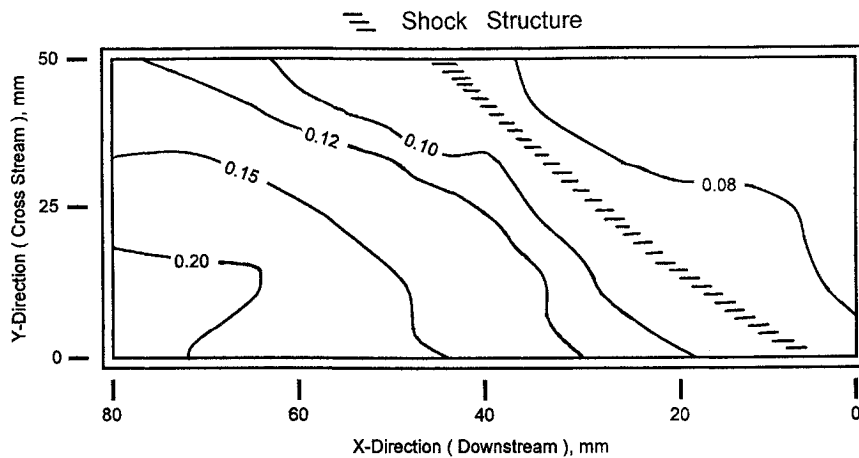


Fig. 3 Contours of constant hue showing the location of a shock at time $T + \Delta T$.

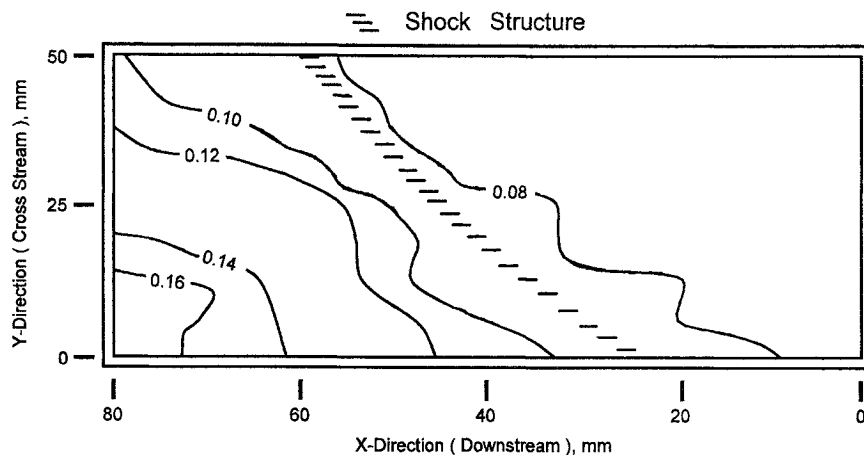


Fig. 4 Contours of constant hue showing the location of a shock line at time $T + 2\Delta T$.

Conclusions

In summary, a simple effective way for determining the starting transients in an intermittent supersonic wind tunnel has been shown. Liquid crystals of the Cholesteric type were used to observe the passing of the starting shock through the test section of a supersonic tunnel and included determination of its propagation velocity. This method of using liquid crystals may be applied and used both from a qualitative and quantitative viewpoint.

Acknowledgment

The authors would like to thank Hallcrest for its guidance and assistance in providing liquid crystals capable of withstanding the wall shear stress in this wind-tunnel facility.

References

- ¹Reda, D. C., and Muratore, J., Jr., "A New Technique for the Measurement of Surface Shear Stress Vectors Using Liquid Crystal Coatings," AIAA Paper 94-0729, Jan. 1994.
- ²Holmes, B. J., Gall, P. D., Croom, C., Manuel, G. S., and Kelliher, W. C., "A New Method for Laminar Boundary Layer Transition Visualization in Flight-Color Changes in Liquid Crystals Coatings," NASA TM-87666, Jan. 1986.
- ³Smith, S. C., "The Use of Liquid Crystals for Surface Flow Visualization," AIAA Paper 90-1382, June 1990.
- ⁴Reda, D. C., and Aeschliman, D. P., "Liquid Crystal Coatings for Surface Shear Stress Visualization in Hypersonic Flows," *Journal of Spacecraft and Rockets*, Vol. 29, No. 2, 1992, pp. 155-158.
- ⁵Toy, N., Savory, E., and Disimile, P. J., "Determination of Surface Temperature and Surface Shear Stress Using Liquid Crystals," 1st ASME/JSME Fluids Engineering Conference, Forum on Turbulent Flows, FED-Vol. 112, American Society of Mechanical Engineers, Portland, OR, June 1991, pp. 39-44.
- ⁶Toy, N., Savory, E., Hoang, Q. H., and Gaudet, L., "Calibration and Use of Shear Sensitive Liquid Crystals in Aerodynamic Testing," *Proceedings of the 15th International Congress on Instrumentation in Aerospace Simu-*

lation Facilities (St. Louis, France), ICIASF Record 93CH3199-7, Inst. of Electrical and Electronics Engineers, New York, 1993, pp. 49.1-49.6.

Sensitivity of Flutter Response of a Wing to Shape and Modal Parameters

Jason Cherian Issac* and Rakesh K. Kapania[†]
Virginia Polytechnic Institute and State University,
Blacksburg, Virginia 24061-0203
 and
 Jean-Francois M. Barthelemy[‡]
NASA Langley Research Center,
Hampton, Virginia 23681

Introduction

AUTOMATIC differentiation is emerging as a valuable tool for sensitivity calculations. ADIFOR, GRESS, PADRE-2, power calculus, and ODYSSEY are some of the automatic differentiation

Received Feb. 1, 1995; revision received May 30, 1995; accepted for publication June 2, 1995. This paper is declared a work of the U.S. Government and is not subject to copyright protection in the United States.

*Graduate Research Assistant, Aerospace and Ocean Engineering. Student Member AIAA.

[†]Professor, Aerospace and Ocean Engineering. Associate Fellow AIAA.

[‡]Assistant Head, Multidisciplinary Design Optimization Branch, Fluid Mechanics and Acoustics Division, MS 159. Senior Member AIAA.